The Formation of Colloidal Crystals of Lipid A Diphosphate: Evidence for the Formation of Nanocrystals at Low Ionic Strength

Chester A. Faunce, Hendrik Reichelt, and Henrich H. Paradies*

Joule Physics Laboratory, Institute for Materials Research, The University of Salford, Manchester M5 4WT, U.K.

P. Quitschau,† V. Rusch,§ and K. Zimmermann§

Department of Chemistry and Chemical Engineering, University of Paderborn, Warburgerstrasse 100, D-33095 Paderborn, Germany

Received: April 15, 2003; In Final Form: June 24, 2003

Dilute electrostatically stabilized aqueous solutions of hexa-acylated (C_{14}) lipid A diphosphate from *Escherichia coli* form stable and regularly shaped colloidal crystals in a size range of approximately 50−1000 nm in width and 50−100 nm in thickness. The formation of these nanocrystals occurs over a range of volume fractions between 3.5×10^{-3} and 1.2×10^{-2} and at a low ionic strength, $\sim 10^{-5}$. The shape of these crystals appears to be cubic or rhombohedral, and when exposed to the electron beam, these fragile nanocrystals are easily damaged. Electron diffraction patterns obtained from single particles reveal that they are orientated (001) crystals that conform to a trigonal or hexagonal unit cell ($a = 3.65 \pm 0.07$ nm and $c = 1.97 \pm 0.04$ nm), revealing crystal-like pore walls that exhibit structural periodicity with a spacing of 0.65 nm and are at least four times the size of the unit cell adopted by lipid A diphosphate.

Lipid A diphosphate, the abundant component of bacterial lipopolysaccharides (LPS), is a glycolipid that is found on the surface of Gram-negative bacteria, is the major component of the outer leaflet of the outer membrane of bacteria, and is well conserved among bacteria. The surface components, LPS, and lipid A diphosphate of many enteric bacteria are also responsible for the virulence. The molecule is of great importance because it provides the host (i.e., humans) with a defense against infection by microorganisms but can also give rise to the development of lethal endotoxic shock.[1] Therefore, the physical structures of lipid A diphosphate are of more than passing interest to future vaccine therapy because of the length, structure, and number of chiral acyl chains linked to the disaccharide units.[2] Compounds known to bind to LPS or lipid A diphosphate do so by multivalent anion binding, which is a chain-length-dependent agglutination of oligosaccharide.[3] Research on lipid A diphosphate molecules will necessarily advance our knowledge of nanoparticle engineering, the behavior of complex fluids,[4] the development of feedstock for pharmaceuticals,[5] and specific biosensors for Gram-negative bacteria.[6]

Monodisperse colloidal particles exhibit a spherically symmetric interaction potential and form colloidal crystals with several different crystal structures depending on the range of their mutual interaction potential.[7] Dispersions of particles exhibiting long-range repulsive interactions undergo an order−disorder transition and if the repulsion between particles is very large, the transition from liquidlike to soft solidlike behavior occurs over a very narrow volume fraction range, assuming low polydispersity.[8] Thus, the interactions between colloidal particles can be tuned by modifying either the particle surfaces or the properties of the matrix in which they are suspended.[9] The repulsive forces increase with decreasing particle−particle separation, particularly for deionized dispersions of charged particles. Unfortunately, a simple method of producing lipid A diphosphate three-dimensional crystals (nanocrystals) or orientated layers of the molecule has yet to be found.

To prepare hexa-acylated lipid A diphosphate (*Escherichia coli*, F-583, Rd mutant) nanocrystals, it was necessary to use electrostatically stabilized solutions (cation-free), and these were obtained only after extensive dialysis.[8] Therefore, very low particle and charge polydispersity is essential in the formation of the nanocrystals. It was noted that upon reaching a nanocluster size of 550 nm the suspension became iridescent; thus, the iridescence acts as a visual marker at this nanocluster size. Under the conditions imposed on the suspensions, nanocrystals of lipid A diphosphate were able to reach sizes of 75 nm and larger. This means that in the formation of nanocrystals particle number density, particle distribution, chemical homogeneity, and purity of the components are of the utmost importance. The details of the procedure to form nanocrystals and ensure equilibrium system conditions, for example, ionic strength, volume fraction, particle size distribution, and pH, are presented in ref 8. The nanocrystals may then be stored either in water or in 0.1 mM NaCl for months without deterioration (25 °C). Both the small and large crystals were analyzed by matrix-assisted laser desorption ionization time of flight mass spectrometry (MALDI-TOF-MS) and liquid chromatography−mass spectrometry (LC-MS) for composition,[8] and no impurities were found to be present. Surprisingly, the presence of 1.0 μM salt improved the lifetime of the nanocrystals. This property was quite unexpected because in the presence of NaCl lipid A diphosphate particles tend to form tight unordered aggregates or water-insoluble precipitates.

Examination of the morphology of the nanocrystals using transmission electron microscopy (TEM, JEOL 3010) and

* To whom correspondence should be addressed. E-mail: Hparadies@aol.com. Phone: (0044)-161-295-3105 or (0049)-2371-566-137. Fax: (0044)-161-295-5147 or (0049)-2371-566-346.

† Present Address: Orthomol GmbH, Elisabeth-Selbert-Strasse 12, D-40764 Langenfeld, Germany.

§ Present Address: Institute for Microecology, Auf den Lüppen 8, D-35745 Herborn, Germany.

10.1021/jp0304428 CCC: $25.00
Published on Web 08/22/2003

scanning electron microscopy (SEM, JEOL 6400) revealed anisometric (platelike) nanoclusters that appeared to be hexagonal or isometric in shape (Figure 1). The microscope images exhibited particles that had adopted a preferred orientation; the majority of the nanocrystals had settled to be coplanar with the TEM support grid. The width of the particles ranged from 50 to 100 nm, and an estimation of the thickness gave a value of ~50.0−100 nm, obtained from assemblies that were located parallel to the electron beam. Neither crystalline structures nor the different appearances of these nanocrystals had been observed for any lipid A diphosphate dispersions.

The powder X-ray diffraction pattern (Bruker XRD diffractometer 5000) obtained from a collection of these nanocrystals (Figure 1D) showed several peaks in the low-angle diffraction region ($2.0° \leq 2\theta \leq 7.5°$), which can be assigned to a hexagonal lattice with lattice constants of $a = 3.85 \pm 0.12$ nm and $c = 1.91 \pm 0.09$ nm, confirming the values of $c = 1.97 \pm 0.035$ nm and $a = 3.68 \pm 0.065$ nm obtained from electron diffraction pattern. The XRD pattern at scattering angles of $7.0° \leq 2\theta \leq 20°$ displays a series of sharp peaks (Figure 1D inset), which can also be indexed on the basis of the hexagonal unit cell. A TEM image (Figure 2A) shows a thin section of a hexagonal close-packed 3-D array of lipid A diphosphate assemblies with a nearest-neighbor spacing of ~3.75 nm. However, we also observed lipid A diphosphate particles that had close-packed multilayers with a lattice spacing of ~2.5 nm. Furthermore, these assemblies show no aggregation and can be stabilized by the addition of 0.5−1.0 μM NaCl (25 °C) and stored for months. A high-resolution TEM image of the assemblies shows that they are ordered and well-separated and that their spacing has been reduced to ~1.0−1.2 nm (Figure 2B). Energy-dispersive X-ray spectrum analysis measurements carried out during the TEM imaging of the specimens confirm that the average nanocrystal of lipid A diphosphate contains both phosphorus (2.87%) and sodium (1.2%). Figure 2C shows a high-resolution TEM micrograph of small lipid A diphosphate crystals. The crystals show a lattice spacing of ~0.65 nm, characteristic of the (111) planes in an ordered fcc structure.

The selected area electron diffraction patterns obtained from various isolated nanocrystalline forms of lipid A diphosphate are shown in Figure 3. The diffraction patterns exhibit hexagonal symmetry, and the reflections display distinct intensity distributions. Figure 3A is consistent with *hk*0 (*hkil*) for $h = 2n$, $k = 2n$, and $l = 3n$ with six molecules in the unit cell on the basis of the measured crystal density and with cell dimensions of $c = 1.97 \pm 0.035$ nm and $a = 3.68 \pm 0.065$ nm (or rhombohedral, $a = 2.25 \pm 0.05$ nm). Other electron diffraction patterns are similar, and they are consistent with $h - k + l \neq 3n$, where the reflections are systematically absent for $l = 0$; hence, the possible enantiomorph space groups are limited to a relatively small number of either hexagonal ($P6_2$, $P6_4$) or centered trigonal groups (R3, *R*32).[9] The apparent 6-fold symmetry could be the result of a 6-fold axis or a 3-fold axis producing, for example, 41.0, $\bar{5}$4.0, and $\bar{1}$5.0, which are equivalent, from Friedel's law where the 41.0 = $\bar{4}\bar{1}$.0. However, it would appear that the nanocrystals have no 2-fold symmetry perpendicular to the 3-fold or 6-fold axis because the pairs of reflection 41.0 and 14.0 or 41.0 and 5$\bar{1}$.0 show equal intensities. In Figure 3B, it can be observed that the electron diffraction pattern has clearly discernible rings consisting of many closely spaced spots indicative of large nanocrystals, and all of these lines correspond to the *hk*0 reflections (sharp diffraction lines). Furthermore, several sharp diffraction rings that correspond to more general *hkl* reflections were observed and were used to determine the *c*

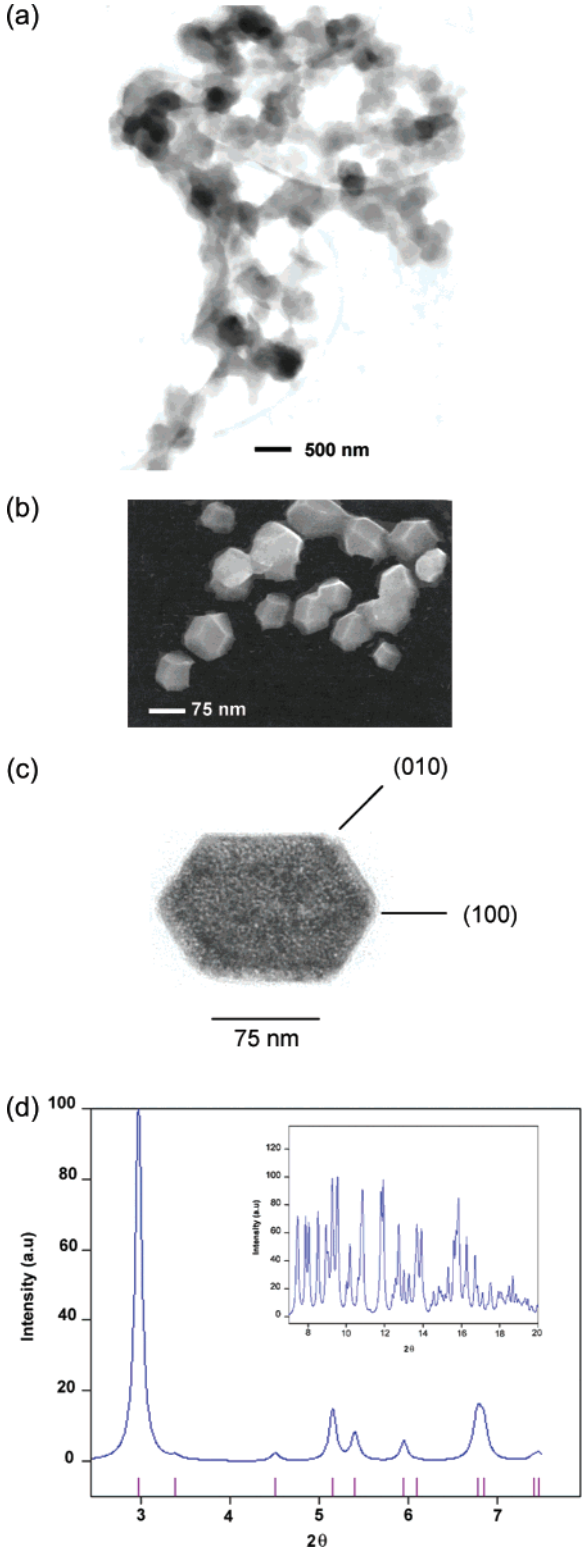

Figure 1. TEM micrograph (A) of a group of nanocrystals of lipid A diphosphate, SEM image (B) of a group of nanocrystals of lipid A diphosphate, TEM micrograph (C) of a single nanocluster of lipid A phosphate. The orientations of the [100] and [010] zone axes were those assumed from selected area electron diffraction. Panel D shows the powder X-ray diffraction patterns of nanocrystals of lipid A diphosphate in the low-angle region ($1.5° \leq 2\theta \leq 5°$) and molecular-scale ($7° \leq 2\theta \leq 20°$) periodic structure. Note that the pattern in the high-angle region is magnified in the inset. The ticks correspond to calculated *d* values assuming a hexagonal unit cell with $c = 1.85$ nm and $a = 3.69$ nm: d_{hkl} (nm) = 1.925 (110), 1.577 (101), 1.22 (201), 1.11 (300), 1.031 (211), 0.963 (220), 0.864 (102), and 0.789 (202).

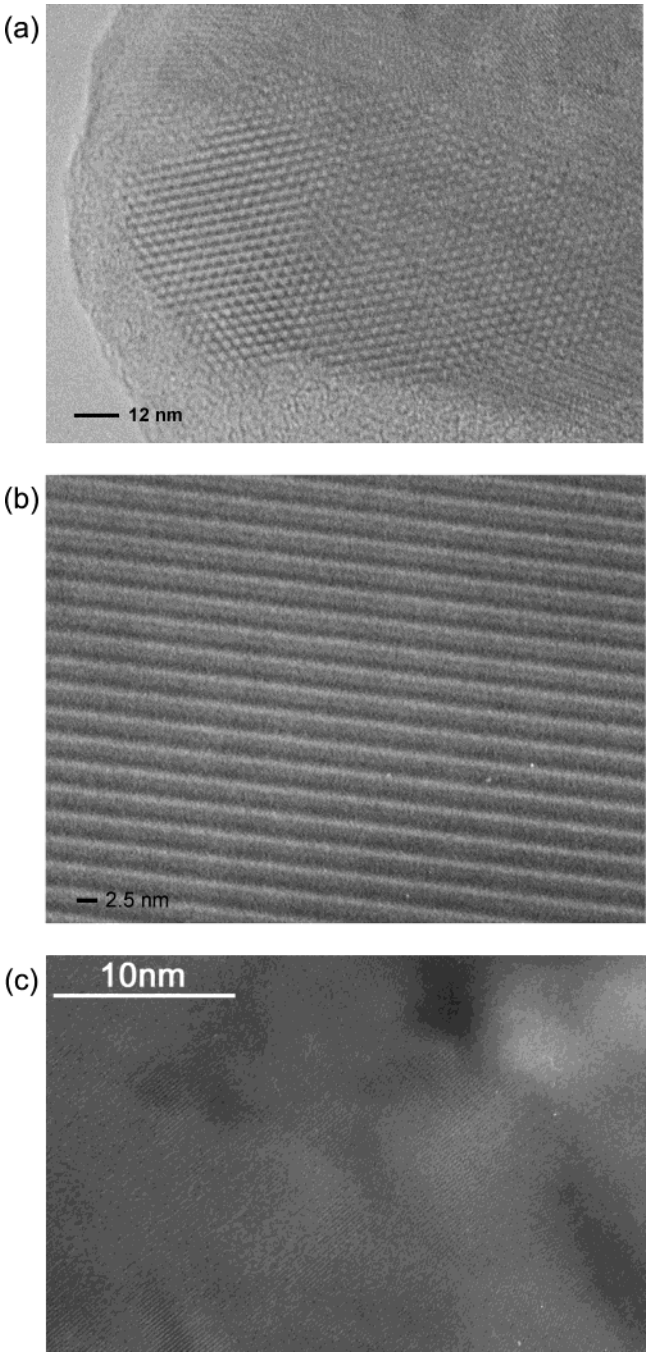

Figure 2. TEM micrograph (A) of a 3D-assembly of lipid A diphosphate on a carbon-coated copper grid (JEOL 3010), high-resolution TEM image (B) of a 10-nm-thick nanocrystalline assembly of lipid A diphosphate, and high-resolution TEM image (C) of 1.0 nm lipid A diphosphate nanocrystals.

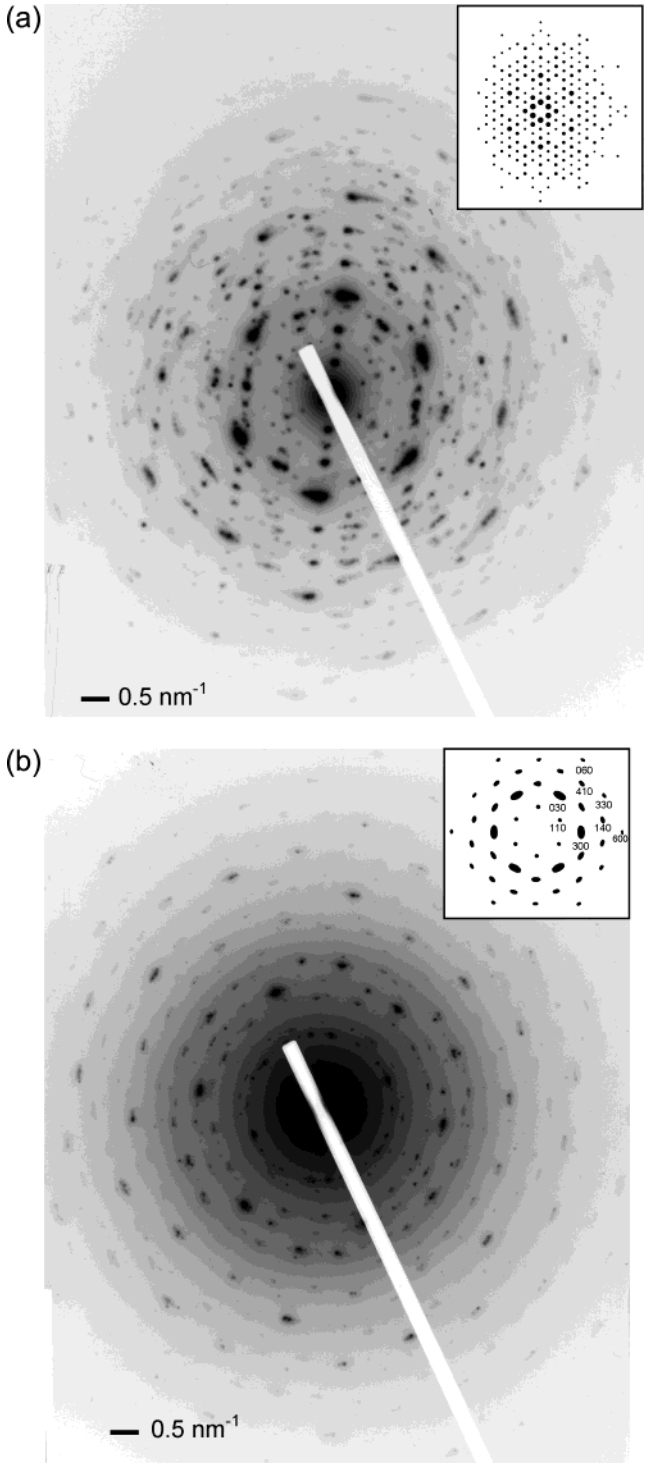

Figure 3. Electron diffraction pattern (A, JEOL 3010, 300 keV, 100 cm) of a 15.0-nm-thick single crystal of lipid A diphosphate. The 6-fold axis and the absences of some of the reflections of the zero layers, trigonal, or hexagonal lattice are clearly seen. The inset shows the simulation of the electron diffraction pattern assuming a space group *R*32 (rhombohedral axis), tilt angle 1.58°, and azimuth angle $\varphi = 2.5°$ and unit cell dimension of $a = 2.25$ nm. Panel B shows the powder electron diffraction pattern showing spotty *hk*0 reflections. This pattern indicates a hexagonal or centered trigonal unit cell with $c = 1.85$ nm and $a = 3.69$ nm. The inset shows the simulated diffraction pattern of the selected area with $c = 1.85$ Å and $a = 3.65$ nm, tilt angle 1.79°, and azimuth angle $\varphi = 5.15°$.

lattice dimension (Figure 3B). These ring patterns confirmed that $c = 1.96$ nm and $a = 3.69$ nm, which is consistent with the recorded small-angle X-ray diffraction pattern. However, the presence of *hk*0 data in the single-crystal diffraction, as well as in the powder patterns, is significant because it shows that the lipid A diphosphate particles adopt a preferred (001) orientation when deposited on a thin carbon film for viewing in the TEM. It is also conceivable that the symmetry is lower than hexagonal if orientational ordering of the lipid A diphosphate anion is considered.[10]

Preliminary information on the geometry of the hexa-acylated chains was obtained at high TEM magnification where lattice images of the layers of lipid A diphosphate exhibited alternating columns of carbon atoms separated by a mean distance of 0.26 nm in the directions of the alkyl chains (*a* to *b*), which can also be seen in Figure 2C. The angle between adjacent spots ($\angle acb$)

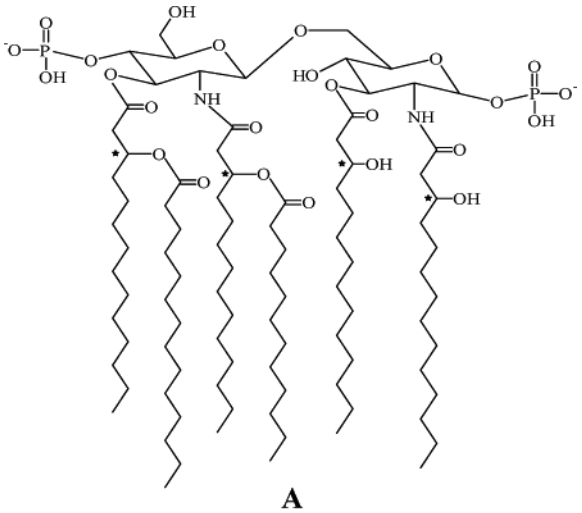

A

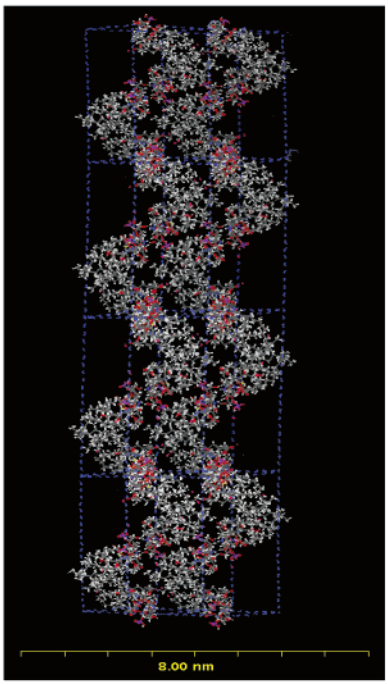

B

Figure 4. Chemical structure (A) of lipid A-diphosphate. Chemically, lipid A diphosphate from *E. coli* consists of a 1,4-diphosphorylated β-1,6-linked D-glucosamine disaccharide with four residues of amide and esterified (*R*)-3-hydroxy fatty acids. Panel B shows the model image of lipid A diphosphate aligned along the 2-fold screw axis, *b*-axis, of the monoclinic unit cell (with $2a = 3.78$ nm, $4b = 7.11$ nm, $c = 3.940$ nm, and $\beta = 62.5°$). The structure was minimized by using the force field COMPASS.[12] Atoms are presented as a stick model: phosphorus violet, oxygen red, carbon black, and hydrogen white.

of an individual molecule was measured to be ~61°, and the distance between these columns was 0.236 nm (*a* to *b* to *c*). Furthermore, the distance between alternating columns in adjacent molecules was 0.296 nm in accord with the X-ray diffraction pattern observed at moderate scattering angles. Figure 4 shows a tentative model of lipid A diphosphate generated on the basis of TEM images and electron diffraction patterns.[11,12] Within the array, crystal-like pores of sizes of ~0.6 nm can be noted that exhibit a structural periodicity with a spacing of 0.65 nm. The periodic pore structure results from hydrophobic alkyl chain layers that are bonded to the disaccharide moiety. Also to be observed in this Figure 4 are lipid A diphosphate molecules orientated along the 2-fold screw axis assuming a monoclinic unit cell.[11] Some of the phosphates are located toward the inner surface area and interact with each other by hydrogen bonding but primarily by the electrostatic interaction potential between phosphate and adjacent phosphate molecules, thus forming the ropes seen in Figure 2C. Moreover, it can be noticed that the hexa-acyl chains are running parallel to each other and separated by ~0.5 nm from each other.

The method described here to produce nanocrystals of lipid A diphosphate appears to have general applications that make it extremely useful for the preparation of other organized lipid A diphosphate assemblies. These assemblies include a variety of penta- and hexa-acylated lipid A diphosphate structures or modifications of the disaccharide moieties such as those of *Enterobacteriaceae*.[13,14]

Acknowledgment. The authors thank Profs. K. D. Ross, S. E. Donnelly, and G. A. Jones and Dr. N. M. Boag for critical discussions and support of this work and Dipl.-Ing. P. Quitschau financial support from the Biomaterials Project (Brussels, Grant BMH4-CT-96-0013).

References and Notes

(1) Raetz, C. R. H.; Whitfield, C. *Annu. Rev. Biochem*. **2002**, *71*, 635. Note: The release of endotoxin is intimately associated with septic shock. This problem caused more than 21 000 mortalities in 1996 in the U.S. alone (*Morbidity and Mortality Weekly Report*; Technical Report No. 46; Center for Disease Control: Atlanta, GA, 1997; pp 941−944).

(2) (a) Hauser, P.; Voet, P.; Sloani, M.; Garcon-Johnson, M.-j.; Desmond, P. U.S. Patent 5,776,468, 1998. (b) Alving, C. R. *Immunology* **1987**, *430*, 1993.

(3) (a) Hayashida, O.; Kato, M.; Akayi, K.; Aoyama, Y. *J. Am. Chem. Soc*. **1999**, *121*, 1597. (b) Li, C.; Budge, L. P.; Driscoll, C. D.; Willardson, B. W.; Allman, G. W.; Savage, P. B. *J. Am. Chem. Soc*. **1999**, *121*, 931.

(4) Tohver, V.; Chan, A.; Sakurada, O.; Lewis, J. A. *Langmuir* **2001**, *17*, 8414.

(5) (a) Felgner, P. L. *Adv. Drug Delivery Res*. **1990**, 5, 163. (b) Weber, M.; Möller, K.; Welzeck, M.; Schorr, J. In *Artifical Self-Assembling Systems for Gene Delivery*; Felgner, P. L., Heller, M. J., Lehn, P., Behr, J. P., Szoka, Fr. C., Eds.; American Chemical Society: Washington, DC, 1996; pp 56−62.

(6) Chan, S.; Horner, S. R.; Fauchet, P. M.; Miller, B. J. *J. Am. Chem. Soc*. **2001**, *123*, 11797.

(7) (a) Hansen, J.-P.; McDonald, L. R. *Theory of Simple Liquids*; Academic Press: New York, 1976. (b) Porn, W.; Pusey, P. N.; Lekkerkerker, H. *Phys. World* **1996**, *9*, 27. (c) Murray, C.; Kagan, C. R.; Bawendi M. G. *Science* **1995**, *220*, 1335. (d) Quesada-Perez, M.; J. Callejas-Fernandez, J. R.; Hidalgo-Alvarez, R. *Phys. Rev. E* **2000**, *61*, 574. (e) Verlet, L.; Hansen, J.-P. *Phys. Rev*. **1984**, *A30*, 999. (f) van Roij, R. *Phys. Rev*. **1984**, *A30*, 999.

(8) (a) Thies, M.; Quitschau, P.; Zimmermann, K.; Rusch, V.; Faunce, C. A.; Paradies, H. H. *J. Chem. Phys*. **2002**, *116*, 3471. (b) Faunce, C. A.; Paradies, H. H.; Quitschau, P. *J. Phys. Chem. B* **2003**, *107*, 2214.

(9) (a)Lekkerkerker, H. N. W.; Stroobants, A. *Nature* **1998**, *393*, 305. (b) Adams, M.; Dogic, Z.; Keller, S. L.; Fraden, S. *Nature* **1998**, *393*, 305.

(10) Henry, N. F. M., Lonsdale, K., Eds., *International Tables for X-ray Crystallography*; The Kynoch Press: Birmingham, U.K., 1965; Vol. 1.

(11) Monoclinic symmetry is required for the lipid A diphosphate anion if the anion is completely orientationally ordered. By lowering the symmetry from cubic to rhombohedral, feasible space groups for the anions are *P*2 or $P2_1$ with $a = 1.89$ nm, $b = 1.777$ nm, $c = 3.940$ nm, and $\beta = 62.5°$, as indicated by very recent X-ray powder diffraction studies (unpublished results).

(12) *Cerius-2 Molecular Simulation Package*, version 4.0; Accelrys: San Diego, CA and Cambridge, U.K., 1999.

(13) (a) Nummila, K.; Kilpelainen, I.; Zähringer, U.; Vaara, M.; Helander, I. M. *Mol. Microbiol*. **1995**, *16*, 271. (b) Hashimoto, M.; Kirikae, F.; Dohi, T.; Adachi, S.; Kusumoto, S.; Suda, Y.; Fujita, T.; Naoki, H.; Kirikae, T. *Eur. J. Biochem*. **2002**, *269*, 3715.

(14) (a) Paradies, H. H.; Zimmermann, K.; Rusch, V. U.S. Patent Application 60/263,494, 2001. (b) Faunce, C. A.; Quitschau, P.; Thies, M.; Scheidt, T.; Paradies, H. H. *Old Herborn University Seminar on Probiotics: Bacteria & Bacterial Fragments as Immunomodulatory Agents*; Herborn Litterae: Herborn, FRG, 2002; Vol. 15, pp 95−120.